The Serpin SQN-5 Is a Dual Mechanistic-Class Inhibitor of Serine and Cysteine Proteinases†

May Al-Khunaizi,‡,§ Cliff J. Luke,‡,§ Yuko S. Askew,‡ Stephen C. Pak,‡ David J. Askew,‡ Sule Cataltepe,‡ David Miller,‡ David R. Mills,‡ Christopher Tsu,‡ Dieter Brömme,|| James A. Irving,⊥ James C. Whisstock,⊥ and Gary A. Silverman*,‡

Department of Pediatrics, The Harvard Medical School, Children's Hospital, 300 Longwood Avenue, Enders 970, Boston, Massachusetts 02115, Department of Human Genetics, Mount Sinai School of Medicine, Fifth Avenue at 100th Street, New York, New York 10029, and Department of Biochemistry and Molecular Biology, Monash University, Melbourne, Victoria 3800, Australia

Received December 3, 2001; Revised Manuscript Received January 10, 2002

ABSTRACT: SQN-5 is a mouse serpin that is highly similar to the human serpins SCCA1 (SERPINB3) and SCCA2 (SERPINB4). Previous studies characterizing the biochemical activity of SQN-5 showed that this serpin, like SCCA2, inhibited the chymotrypsin-like enzymes mast cell chymase and cathepsin G. Using an expanded panel of papain-like cysteine proteinases, we now show that SQN-5, like SCCA1, inhibited cathepsins K, L, S, and V but not cathepsin B or H. These interactions were characterized by stoichiometries of inhibition that were nearly 1:1 and second-order rate constants of $>10^4$ M^{-1} s^{-1}. Reactive site loop (RSL) cleavage analysis showed that SQN-5 employed different reactive centers to neutralize the serine and cysteine proteinases. To our knowledge, this is the first serpin that serves as a dual inhibitor of both chymotrypsin-like serine and the papain-like cysteine proteinases by employing an RSL-dependent inhibitory mechanism. The ability of serpins to inhibit both serine and/or papain-like cysteine proteinases may not be a recent event in mammalian evolution. Phylogenetic studies suggested that the SCCA and SQN genes evolved from a common ancestor approximately 250−280 million years ago. When the fact that mammals and birds diverged approximately 310 million years ago is considered, an ancestral SCCA/SQN-like serpin with dual inhibitory activity may be present in many mammalian genomes.

On the basis of their well-conserved tertiary structure and suicide substrate-like mechanism of inhibition, the serpins[1] occupy a unique niche among the diverse groups of active site-directed proteinase inhibitors (reviewed in ref *1*). Most serpins inhibit trypsin-like enzymes of the *clan SA* [MEROPS, The Protease Database (http://www.merops.ac.uk/merops/index.htm)]. A few serpins inhibit different types of cysteine proteinases as well. For example, the viral serpin, CrmA, and the human serpin, SERPINB9 (PI9), inhibit caspase 1 (*clan CD*) (*2*, *3*), and a bovine antichymotrypsin-like serpin inhibits a novel (unclassified) prohormone thiol protease (*4*). More recently, we showed that the human squamous cell carcinoma antigen 1 [SCCA1 (SERPINB3)] inhibits members of the papain family of cysteine proteinases (*clan CA*), cathepsins K, L, and S (*5*). Inhibition was dependent on the SCCA1 reactive site loop (RSL), suggesting that serpins employ their unique suicide substrate-like mechanism to inhibit both cysteine and serine proteinases (*6*).

SCCA2 (SERPINB4) is 92% identical to SCCA1 at the amino acid level (*7*). The genes are tandemly arrayed in a head-to-tail orientation with SCCA2 lying less than 10 kb centromeric to SCCA1 (*7*). The major differences between SCCA1 and SCCA2 are eight residues that reside in the RSL. This difference suggested that SCCA2 would inhibit proteinases different than those neutralized by SCCA1. To an extent, this was the case as SCCA2 inhibits the chymotrypsin-like proteinases catG and mast cell chymase (*8*). However, SCCA2 also inhibited catS, albeit with a second-order rate constant that was 50-fold lower than that of SCCA1 (*9*). Via mutation of the P1, P3′, P4′, and P11′ residues of the RSL of SCCA2 to those present in the RSL of SCCA1, the rate of catS inhibition by SCCA2 increased to 80% of that observed for the SCCA1−catS interaction (*9*). Collectively, these findings suggested that an ancestral SCCA-like gene inhibited both serine and cysteine proteinases and that the recent duplication of the SCCA locus in mammals allowed for the separation and specialization of these two different inhibitory activities.

† This work was supported by grants form the NCI (CA87006 and CA86002) and NICHD (HD07466).

* To whom correspondence should be addressed: Children's Hospital, 300 Longwood Ave., Enders 970, Boston, MA 02115-5737. Telephone: (617) 355-6416. Fax: (617) 355-7677. E-mail: gary.silverman@tch.harvard.edu.

‡ The Harvard Medical School.

§ These authors contributed equally to this work.

|| Mount Sinai School of Medicine.

⊥ Monash University.

[1] Abbreviations: serpin, serine proteinase inhibitor; RSL, reactive site loop; cat, cathepsin; HNE, human neutrophil elastase; uPA, urokinase-type plasminogen activator; SCCA1 and -2, squamous cell carcinoma antigen 1 and 2, respectively; GST, glutathione *S*-transferase; succ-AAPF-pNA, succinyl-Ala-Ala-Pro-Phe-*p*-nitroanilide; $(Z\text{-PR})_2$-R110, (benzyloxycarbonyl-Pro-Arg)$_2$-R110; $(Z\text{-FR})_2$-R110, $(Z\text{-Phe-Arg})_2$-R110; SI, stoichiometry of inhibition; MALDI-MS, matrix-associated laser desorption ionization mass spectroscopy; MYA, million years ago.

10.1021/bi015999x CCC: $22.00
Published on Web 02/07/2002

Although SCCA1 and SCCA2 serve as circulating tumor markers for several types of advanced squamous cell carcinomas, the biologic function of these serpins is still ill-defined (reviewed in ref *10*). Insight into the biologic function of human genes may be obtained by targeted mutagenesis of orthologous genes in mice. As a prelude to this type of approach, we isolated a mouse serpin, SQN-5, with a amino acid sequence that is highly similar to those of SCCA1 and -2 (*11*). *SQN-5* mapped between *Pai2* and *Bcl2* on mouse chromosome 1, a region which is syntenic with the SCCA locus at 18q21.3. The structures of the genes were identical in terms of the number of exons ($n = 8$) and splicing phase (0, 0, 0, 0, 1, 0, 0). Moreover, the tissue expression patterns of SQN-5 and the SCCAs were very similar with the highest amount of expression in the lung, thymus, skin, uterus, and gastrointestinal tract. The reactive center of SQN-5 contained Thr and Ser residues at the putative P1−P1′ site. This motif was more similar to the Ser and Ser of SCCA1 than the Leu and Ser of SCCA2. Nonetheless, preliminary kinetic analysis showed that SQN-5, like SCCA2, inhibited the chymotrypsin-like serine proteinases catG and mast cell chymase with stoichiometries of 1:1 and 2:1 and with second-order rate constants of 1.7×10^5 and 0.9×10^4 M^{-1} s^{-1}, respectively. Using low concentrations of catS, we were unable to detect inhibition using SQN-5. From these data, we concluded that SQN-5 was the murine ortholog of SCCA2. However, recently, we have detected variability in the velocity of substrate conversion using active site-titrated catS prepared from human liver and a recombinant protein isolated from yeast. Also, as noted above, when higher concentrations of SCCA2 and enzyme were used in the assay, SCCA2 exhibited low-level inhibitory activity against catS ($k_a = 2.4 \times 10^3$ M^{-1} s^{-1}) (*9*). For these reasons, we re-examined the ability of SQN-5 to inhibit papain-like cysteine proteinases. Using an expanded panel of papain-like cysteine proteinases, we showed that SQN-5 inhibits catK, -L, -S, and -V but not catB or -H. The stoichiometry of inhibition for these reactions was near 1:1. Unlike that of SCCA2, however, the second-order rate constants for the SQN-5−cysteine proteinase interactions were more comparable to those observed for the SCCA1−cysteine proteinase interactions. These data suggested that SQN-5 and SCCA2 are not orthologs. Rather, SQN-5, the other SQNs, SCCA1, and SCCA2 are paralogous genes, and they may have evolved from an ancestral SCCA/SQN-like gene that encoded a serpin with dual inhibitory activity against serine and cysteine proteinases.

EXPERIMENTAL PROCEDURES

Production of Recombinant SQN-5. A 1.2 kb DNA fragment containing the complete coding sequence of *SQN-5* was ligated into the pGEX-2T bacterial expression vector (Amersham Pharmacia, Uppsala, Sweden) as described previously (*11*). SQN-5 was ligated to the 3′ side of the glutathione *S*-transferase (GST) sequence. The recombinant GST−SQN-5 fusion protein and GST were batch purified using glutathione−Sepharose 4B beads (*8*).

Enzymes, Substrates, and Buffers. Human catG, -B, -H, and -L were purchased from Athens Research & Technology, Inc. (Athens, GA). Recombinant catK, -S, and -V were prepared as described previously (*12*−*14*). Papain was purchased from Sigma (St. Louis, MO).

Table 1: Inhibitory Profile of SQN-5

proteinase (final concentration)	[SQN-5] (nM)	ratio ([I]/[E])	% inhibition[a]	substrate (final concentration)
catB (50 nM)	500	10	0	$(Z\text{-}FR)_2$-R110 (5 μM)
catG (84 nM)	720	9	91	succ-AAPF-pNA (1 mM)
catH (25 nM)	500	20	0	$(Z\text{-}PR)_2$-R110 (5 μM)
catK (30 nM)	500	16	97	$(Z\text{-}FR)_2$-R110 (5 μM)
catL (20 nM)	500	25	95	$(Z\text{-}FR)_2$-R110 (5 μM)
catS (50 nM)	500	10	98	$(Z\text{-}FR)_2$-R110 (5 μM)
catV (25 nM)	500	10	98	$(Z\text{-}FR)_2$-R110 (5 μM)
papain (50 nM)	500	10	35	$(Z\text{-}FR)_2$-R110 (5 μM)

[a] Proteinase and SQN-5 were incubated for 30 min at 25 °C. Residual enzyme activity was measured by adding substrate and assessing its hydrolysis over time. Buffers that were used are listed in Experimental Procedures. Percent inhibition = 100 × [1 − (velocity in the presence of inhibitor/velocity of uninhibited control)].

Enzyme substrates were purchased from Sigma [succinyl-Ala-Ala-Pro-Phe-*p*-nitroanilide (succ-AAPF-pNA)] and Molecular Probes, Inc. (Eugene, OR) {(benzyloxycarbonyl-Pro-Arg)$_2$-R110 [$(Z\text{-}PR)_2$-R110] and $(Z\text{-}Phe\text{-}Arg)_2$-R110 [$(Z\text{-}FR)_2$-R110]}.

PBS [137 mM NaCl, 27 mM KCl, and 10 mM phosphate buffer (pH 7.4)] was used in enzymatic reactions with catG. Cathepsin reaction buffer [50 mM sodium acetate (pH 5.5), 4 mM dithiothreitol, and 1 mM EDTA] was used with the cysteine proteinases.

Determination of Protein Concentrations. The concentrations of the cysteine proteinases were determined by active site titration using the inhibitor L-3-carboxy[(*trans*-2,3-epoxyprolyl)leucyl]amido(4-guanidino)butane (E-64) as described previously (*15*). CatG was calibrated against a standardized concentration of α1-proteinase inhibitor as described previously (*8*). The concentration of recombinant SQN-5 was determined by using Bio-Rad Protein Assay Kit II (Bio-Rad, Hercules, CA).

Screening Assays for Enzyme Inhibition. The screening for SQN-5 inhibitory activity was determined by mixing enzyme and inhibitor in the appropriate buffer, incubating for 30 min at 25 °C, and measuring the residual enzyme activity as described previously (*8*). Residual enzyme activity was determined by adding the appropriate substrate and assessing its hydrolysis over time (velocity) using either a THERMOmax (in the case of the -pNA substrate) or *f*max (in the case of -R110 substrates) microplate reader (Molecular Devices, Sunnyvale, CA). For the UV−visible substrate, -pNA, a wavelength of 405 nm was used. For the fluorescent substrate, -R110, the excitation and emission spectra were recorded at 485 and 538 nm, respectively. The concentrations of enzyme, inhibitor, and substrate are listed in Table 1, and the buffers are listed above. Percent enzyme inhibition = 100 × [1 − (velocity of inhibited enzyme reaction/velocity of uninhibited enzyme reaction)].

Binding Stoichiometries. Assays for binding between SQN-5 and the cysteine proteinases (range of 15−25 nM) or catG (50 nM) were performed in a volume of 100 μL in 96-well microtiter plates (Costar 9017, Costar, Cambridge, MA). The inhibitor (concentration range of 0−50 nM) was incubated with the enzyme for 20−30 min at 25 °C. The -R110 and -pNA substrates were added to final concentrations of 5 μM and 1 mM, respectively. The velocity of substrate hydrolysis was measured using the appropriate microplate reader. The partitioning ratio of the inhibitor−

enzyme association was determined by plotting the fractional activity (velocity of the inhibited enzyme reaction/velocity of the uninhibited enzyme reaction) versus the ratio of the inhibitor to enzyme ($[I]_0/[E]_0$) (*15*). The *x*-intercept [i.e., the stoichiometry of inhibition (SI)] was determined by linear regression analysis.

Enzyme Kinetics. The interactions of SQN-5 with the cysteine proteinases were determined by the progress curve method (*16*). Under these pseudo-first-order conditions, a constant concentration of enzyme (10−25 nM) was mixed with different concentrations of inhibitor (0−1660 nM) and substrate (final concentration of 5 μM). The rate of product formation was measured using the microplate reader. Since the inhibition of the enzymes is assumed to be irreversible over the course of the reaction, product formation is described as shown below, where the amount of product formation (P) proceeds at an initial velocity (υ_z) and is inhibited over time (t) at a rate k_{obs}:

$$P = \upsilon_z/k_{obs} \times (1 - e^{-k_{obs}t}) \quad (1)$$

For each combination of enzyme and inhibitor, a k_{obs} was calculated by nonlinear regression of the data using eq 1. A second-order rate constant (k') was determined by plotting a series of k_{obs} values versus the respective inhibitor concentration and measuring the slope of the line ($k' = \Delta k_{obs}/\Delta[I]$).

Since the inhibitor is in competition with the substrate and the rate depends on the SI, the second-order rate constant (k') was corrected for the substrate concentration, the SI of the enzyme and inhibitor, and the K_m of the enzyme for the substrate to calculate the k_a as shown:

$$k_a = k'(1 + [S]/K_m) \times SI \quad (2)$$

The K_m values of catK, -L, -S, and -V for $(Z\text{-}FR)_2$-R110 in cathepsin buffer were 4, 2, 8, and 13.5 μM, respectively. Assays were repeated at least three times and were reported ±1 standard deviation of the mean.

The association rate constants for the interactions of catG with SQN-5 were determined under second-order conditions (*17*). Equimolar amounts (50 nM) of enzyme and inhibitor were incubated at 25 °C for varying periods of time. The reaction was quenched by the addition of excess substrate (final volume of 110 μL), and the velocity of the free enzyme activity was measured using a microplate reader. The velocity was converted to free enzyme concentration using an enzyme concentration standard curve. The rate of change in the amount of free enzyme over time is described in eq 3, where the slope of the plot of the reciprocal of the remaining free enzyme ($1/E_f$) over time (t) yields a second-order rate constant (k_a):

$$1/E_f = k_a t + 1/E_0 \quad (3)$$

The *y*-intercept of this plot is the reciprocal of the initial enzyme concentration (E_0).

SDS−PAGE and Immunoblotting. SQN-5 (5 μg) or SCCA1 (positive control) was incubated with catL (1.6 μg) for 10 min at 25 °C. Samples were mixed with 3× Laemmli sample buffer [2% SDS, 25% glycerol, 62.5 mM Tris-HCl (pH 6.8), and 0.01% bromophenol blue], heated to 95 °C for 5 min, and separated by SDS−PAGE (8% acrylamide, 19:1 T:C ratio) according to the method of Laemmli (*18*). The running buffer (pH 8.3) was 25 mM Tris-base, 250 mM glycine, and 0.1% SDS. Protein bands were visualized after staining in a solution containing 0.25% Coomassie Brilliant Blue R-250, 45% methanol, and 10% acetic acid. For immunodetection, proteins separated by SDS−PAGE were electroblotted at 100 V for 1 h at 4 °C onto reinforced nitrocellulose (NitroPure, Osmonics Inc., Westborough, MA) as described previously (*19*). The transfer buffer was 25 mM Tris-base (pH 8.0) and 190 mM glycine (pH 8.3). Serpin−catL complexes were detected using a rabbit polyclonal catL antiserum diluted 1:1000 as the primary antibody (Athens Research & Technology, Inc.) and a horseradish peroxidase-linked anti-rabbit antibody (Amersham Pharmacia Biotech) diluted 1:2500 as the secondary antibody. The immunoblot was visualized using the ECL detection kit (Amersham Pharmacia Biotech).

Matrix-Associated Laser Desorption Ionization Mass Spectroscopy (MALDI-MS). For catG, 2 μM proteinase in PBS reaction buffer was mixed with 2 μM SQN-5 for 5 min at 25 °C. For the cysteine proteinases, 1.2 μM enzyme in cathepsin buffer was mixed with 12 μM SQN-5. The mixture components were separated by MALDI-MS at the Wistar Protein Microchemistry Facility (Philadelphia, PA).

Construction of the ov-Serpin Phylogenetic Tree. The 13 human ov-serpins along with their mouse orthologs were obtained from GENPEPT and aligned with SQN-5, SQN-LS, SQN-RS, and SQN-2 (the latter three mouse sequences are unpublished, from D. Askew and G. Silverman) using CLUSTALW (*20*). Minor adjustments were made to the alignment to take into account elements of secondary structure (*21*). Bootstrapping (1000 trials) was performed using CLUSTALW, and the phylogenetic tree was constructed using NJPLOT (*22*).

RESULTS

Inhibition of Serine and Cysteine Proteinases by SQN-5. Previous biochemical studies using SQN-5 showed that this serpin inhibited the chymotrypsin-like enzymes mast cell chymase and catG with binding stoichiometries near 1:1 (*11*). To ensure that the batch of SQN-5 prepared for these studies had comparable activity, the serpin was mixed with catG and substrate and assayed for the stoichiometry of inhibition (SI, described below) and inhibitory activity (Table 1 and Figure 1). As expected, SQN-5 neutralized catG with a stoichiometry near 1:1 (Figure 1A) and inhibited the enzyme under second-order conditions with a second-order rate constant (k_a) of 1×10^5 M^{-1} s^{-1} (Figure 1B). This value was comparable to that measured in the previous study [$k_a = 1.7 \times 10^5$ M^{-1} s^{-1} (*11*)].

Next, we examined the ability of SQN-5 to inhibit papain-like cysteine proteinases. This study was prompted by a re-examination of the amino acid sequence of SQN-5's RSL and consideration of the substrate specificities for the papain-like cysteine proteinases. In part, the specificity of serine proteinases is determined by which residues can be accommodated at the S1 subsite (i.e., the P1 residue of the substrate). In contrast, the specificity of papain-like cysteine proteinases is governed by residues capable of binding to the S2 subsite, with Leu, Val, and Phe being the more preferred P2 residues for catL and catS and Arg for catB

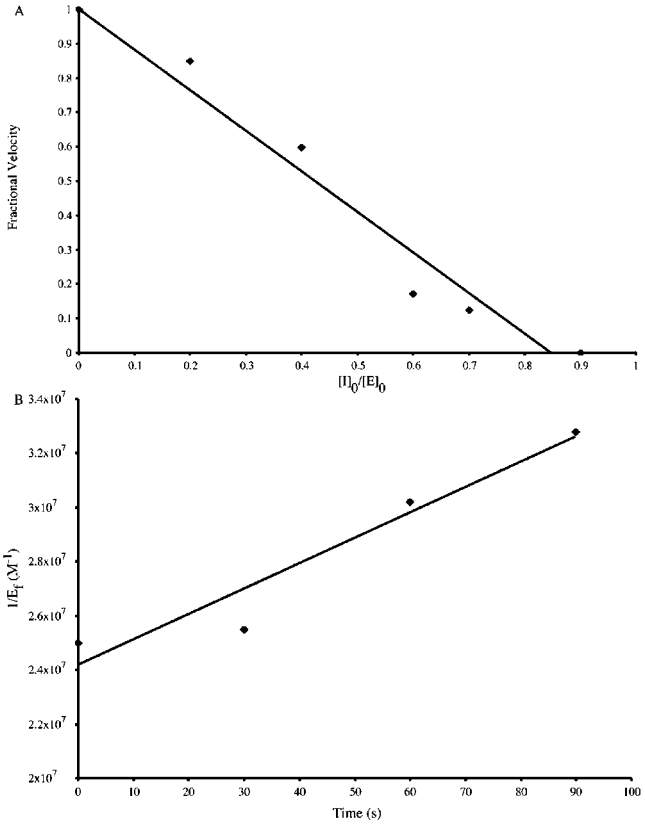

FIGURE 1: Inhibition of cathepsin G by SQN-5. (A) Stoichiometry of inhibition. CatG (100 nM) was incubated with varying amounts of SQN-5 (0−100 nM) at 25 °C for 30 min in PBS. The residual activity was measured by the addition of succ-AAPF-pNA substrate (final concentration of 1 mM) and measuring the absorbency at 405 nm in a microplate reader. The stoichiometry was determined by plotting the fractional velocity over the ratio of initial inhibitor concentration to initial enzyme concentration ($[I]_0/[E]_0$). Fractional activity was determined by the ratio of the velocity of the inhibited enzyme (v_I) to the velocity of the uninhibited enzyme (v_0). The stoichiometry was determined using linear regression analysis to extrapolate the $[I]_0/[E]_0$ ratio that resulted in 100% inhibition. (B) Inhibition of catG by SQN-5 under second-order conditions. Equimolar concentrations (100 nM) of catG were incubated at 25 °C in PBS. Aliquots (100 μL) were removed at different time points, and the reactions were quenched by the addition of 100 mM succ-AAPF-pNA (10 μL). Residual activity was measured by the velocity of substrate hydrolysis at 405 nm in the microplate reader. The free enzyme concentration (E_f) was determined using a standard curve of catG (0−100 nM). The association rate (k_a) was the slope of the line obtained from plotting the reciprocal of the free enzyme concentration ($1/E_f$) over time. The calculated second-order rate constant (k_a) for SQN-5 and catG was 1×10^5 M^{-1} s^{-1}.

(*12*). Although SQN-5 has Thr and Ser residues at the putative P1 and P1′ positions, respectively, a Leu residue at the P2 position makes SQN-5 a potential inhibitor for some papain-like cysteine proteinases. When excess SQN-5 was mixed with various papain-like cysteine proteinases and their appropriate substrates, inhibition of catK, -L, -S, and -V was detected (Table 1). There was no inhibition of catB or -H.

Although these studies suggested that SQN-5 inhibited catK, -L, -S, and -V, the nature of the assay did not permit discrimination between true serpin-like inhibitory activity versus simple competition between the reporter substrate and SQN-5. If SQN-5 was a true inhibitor rather then a simple substrate for catK, -L, -S, and -V, the interaction would occur (1) with a stoichiometry near 1:1, (2) with a second-order

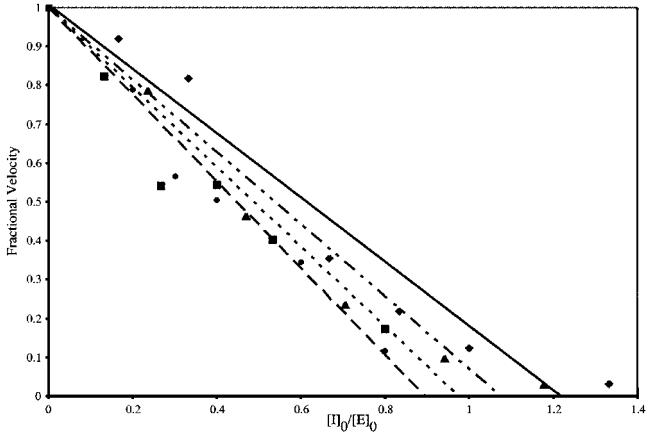

FIGURE 2: Stoichiometry on SQN-5−cysteine proteinase inhibition. Varying concentrations of SQN-5 (0−50 nM) were incubated with catK (15 nM) (■), catL (17 nM) (▲), catS (50 nM) (◆), and catV (25 nM) (●) at 25 °C for 20 min in cathepsin buffer (pH 5.5). The residual activity was measured by the addition of the $(Z\text{-}FR)_2$-R110 substrate (final concentration of 5 μM) and measuring the fluorescence at an excitation wavelength of 485 nm and an emission wavelength of 538 nm in a microplate reader. The stoichiometry was determined by plotting the fractional velocity over the ratio of initial inhibitor concentration to initial enzyme concentration ($[I]_0/[E]_0$). Fractional activity was determined by the ratio of the velocity of the inhibited enzyme (v_I) to the velocity of the uninhibited enzyme (v_0). The stoichiometry was determined using linear regression analysis [catK (− − −), catL (- − -), catS (—), and catV (- - -)] to extrapolate the $[I]_0/[E]_0$ ratio that resulted in 100% inhibition.

rate constant of $\geq 10^4$ M^{-1} s^{-1}, and (3) via RSL cleavage and the formation of a covalent−acyl enzyme complex.

Stoichiometry of Inhibition. The interaction between an inhibitory-type serpin and its target proteinase usually results in the formation of a covalent complex (inhibitory pathway, with a rate k_i), but parallel substrate reactions can occur (substrate pathway, with a rate k_s) (*23*). The extent to which the serpin−proteinase complexes partition down these pathways is reflected in the stoichiometry of inhibition (SI), where the $SI = (k_s + k_i)/k_i$. If the substrate pathway predominates over the inhibitory pathway, the SI will exceed 1, whereas in the absence of the substrate reaction, the SI = 1 (*24*). The SI for a serpin proteinase reaction is determined by titration of the proteinase with the inhibitor and extrapolating to the $[I]_0/[E]_0$ ratio that results in a complete loss of enzyme activity. When various amounts of SQN-5 were incubated with catK, -L, -S, or -V, the SIs for all of these interactions were ~1 (Figure 2).

Rate of Complex Formation. To determine the rate of complex formation between SQN-5 and either catK, -L, -S, or -V, we performed a kinetic analysis under first-order conditions using the progress curve method (*16*). CatK, -L, -S, or -V was incubated with an excess of SQN-5 in the presence of substrate. The progress of enzyme inactivation was followed and represented as a simple decay with a rate k_{obs} (eq 1). Rate constants (k_{obs}) obtained at different concentrations were plotted against the inhibitor concentrations, and the slope of this line (k') and the K_m of the substrate were used to calculate the overall second-order rate constant (k_a) as described by eq 2. The k_a values for the interaction between catK, -L, -S, and -V and SQN-5 were (5.9 ± 0.3), (8.2 ± 5.0), (4.2 ± 0.2), and (12.6 ± 3.6) × 10^4 M^{-1} s^{-1}, respectively (Figure 3).

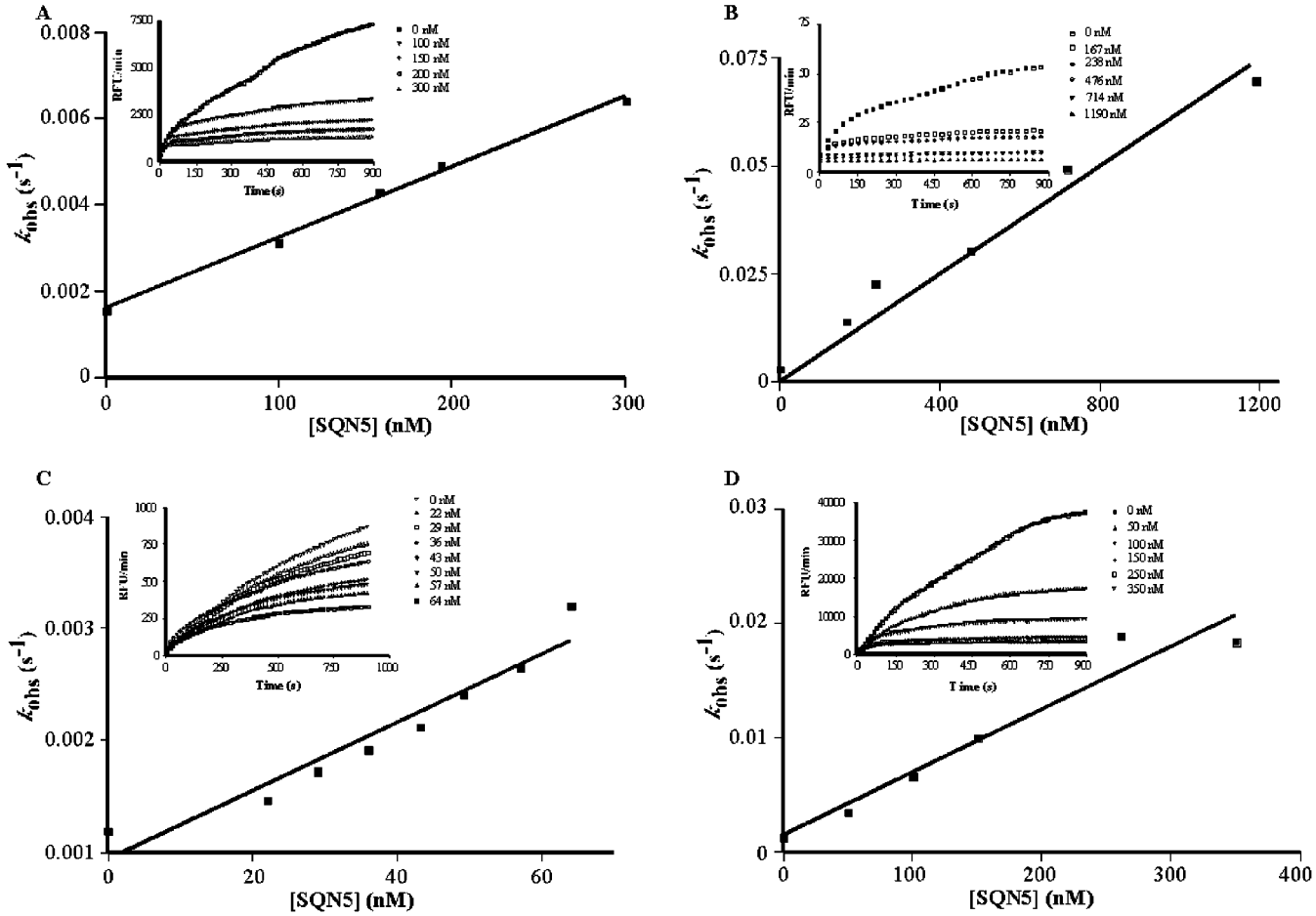

FIGURE 3: Rates of SQN-5−cysteine proteinase interactions. The interactions between SQN-5 and catK (A), catL (B), catS (C), and catV (D) were measured under pseudo-first-order conditions using the progress curve method. CatK (15 nM), catL (17 nM), catS (2 nM), and catV (25 nM) and substrate $(Z\text{-}FR)_2$-R110 (5 μM final concentration) were added to varying amounts of SQN-5 (0−1190 nM). The progress of inactivation of the different cathepsins at different concentrations of the inhibitor in cathepsin buffer (pH 5.5) was followed by measuring the fluorescence with an excitation wavelength of 485 nm and an emission wavelength of 538 nm every 15 s. Representative progress curves for each cathepsin are shown in the insets. If an irreversible reaction is assumed, the first-order rate constant (k_{obs}) was calculated using a nonlinear regression fit of each curve using eq 1. A second-order rate constant (k') was obtained from the slope of the k_{obs} over the concentration of the inhibitor. Accounting for the K_m of the enzyme and substrate, corrected second-order rate constants (k_a) were calculated using eq 2. The k_a values for catK, -L, -S, and -V were 1.7, 3.6, 3.1, and 7.2 × 10^4 M^{-1} s^{-1}, respectively.

Comparison between the SQN-5 and SCCA1 Interactions with Cathepsin V. To compare directly the cysteine proteinase inhibitory activity of SQN-5 with SCCA1, we measured the second-order rate constant for the SCCA1−catV interaction after first determining that the SI for the interaction was ∼1 (Figure 4A). We also chose this combination since the interaction between SCCA1 and catV had not been previously reported and the interactions of SCCA1 with catK, -L, and -S were already available for comparison (*5*). Using the progress curve method, the k_a for the SCCA1−catV interaction was measured to be 7.9 × 10^4 M^{-1} s^{-1} (Figure 4B). This value is nearly identical to that determined for the SQN-5−catV interaction using the same assay procedure.

A comparison of the second-order rate constants obtained for the SQN-5 and SCCA1 interactions with catK, -L, -S, and -V is given in Table 2. In general, the ability of SQN-5 to inhibit this panel of papain-like cysteine proteinases in vitro is comparable to that of SCCA1.

Complex Formation. Serpins form covalent complexes with their target serine proteinases. Typically, these complexes do not dissociate in the presence of SDS, reducing agents, and heat (*25*). Previous studies using SCCA1 and catS showed that serpins also could form complexes with cysteine proteinases (*5*). Although these complexes were resistant to heating in SDS, they dissociated in the presence of reducing agents. This decreased stability, relative to those of the serpin−serine proteinase complexes, most likely reflects the increased susceptibility of the thiol−ester linkage to reducing agents such as dithiothreitol or β-mercaptoethanol. To determine whether SQN-5 (GST−SQN-5 $M_r \cong$ 71 000) could form a covalent complex with a papain-like cysteine proteinase, the serpin was mixed with catL ($M_r \cong$ 24 000) and then incubated at 95 °C for 2 min in the presence of 2% SDS. Samples were analyzed by SDS−PAGE and immunoblotting with an anti-catL polyclonal antiserum (Figure 5). A band at an M_r of ≅95000 was detected in the expected position for an SQN-5−catL complex. The molecular weight of this complex was similar to that detected for the SCCA1−catL complex (Figure 5). As expected, the presence of β-mercaptoethanol in the loading buffer inhibited complex formation (not shown).

Reactive Center of SQN-5. Due to the mechanism of serpin inhibition, RSL cleavage usually occurs ∼17 residues downstream of the highly conserved Glu residue [P17 based on archetypal serpin, α1-antitrypsin (SERPINA1)] that is located in the proximal hinge region (*26*). To identify the

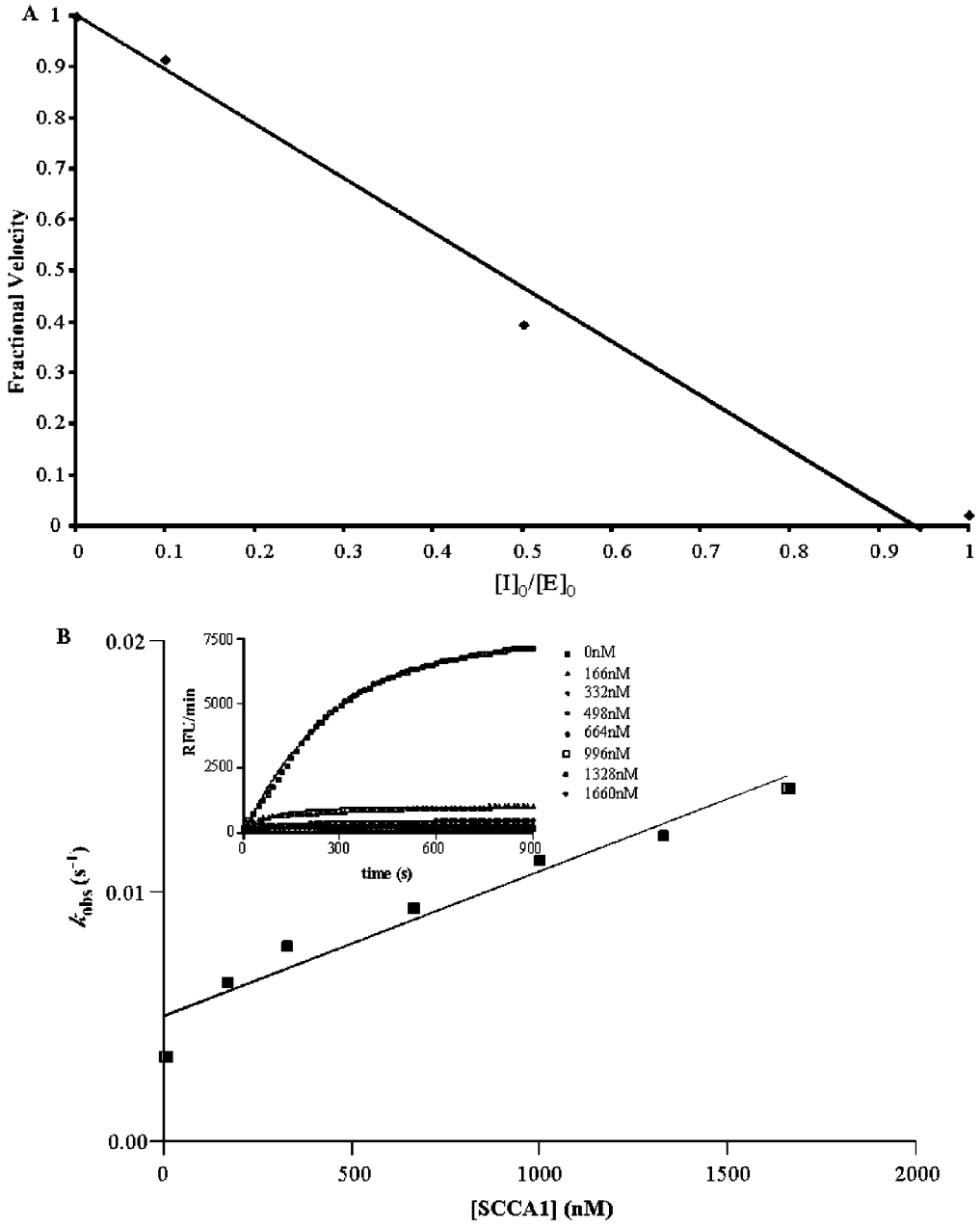

FIGURE 4: SCCA1−catV interactions. (A) Stoichiometry of inhibition for SCCA1 (0−25 nM) and catV (25 nM). Varying concentrations of SCCA1 were incubated with catV at 25 °C for 20 min in cathepsin buffer (pH 5.5). The residual activity was measured by the addition of substrate $(Z\text{-}FR)_2$-R110 (final concentration of 5 μM) and measuring the fluorescence at an excitation wavelength of 485 nm and an emission wavelength of 538 nm in a microplate reader. The stoichiometry was determined by plotting the fractional velocity over the ratio of initial inhibitor concentration to initial enzyme concentration ($[I]_0/[E]_0$). Fractional activity was determined by the ratio of the velocity of the inhibited enzyme (v_I) to the velocity of the uninhibited enzyme (v_0). The stoichiometry was determined using linear regression analysis to extrapolate the $[I]_0/[E]_0$ ratio that resulted in 100% inhibition. (B) The rate of SCCA1−catV interaction was measured under pseudo-first-order conditions using the progress curve method. CatV (25 nM) and substrate $(Z\text{-}FR)_2$-R110 (5 μM final concentration) were added to varying amounts of SCCA1 (0−1660 nM). The progress of inactivation of catV at different concentrations of the inhibitor in cathepsin buffer (pH 5.5) was followed by measuring the fluorescence with an excitation wavelength of 485 nm and an emission wavelength of 538 nm every 15 s. A representative progress curve is shown in the inset. If an irreversible reaction is assumed, the first-order rate constant (k_{obs}) was calculated using a nonlinear regression fit of each curve using eq 1. A second-order rate constant (k') was obtained from the slope of the k_{obs} over the concentration of the inhibitor. Accounting for the K_m of the enzyme and substrate, a corrected second-order rate constant (k_a) was calculated using eq 2. The k_a for the SCCA1−catV interaction was 7.9×10^4 M^{-1} s^{-1}.

reactive center (P1−P1′) for SQN-5, serpin and cysteine proteinases were co-incubated and the resulting C-terminal cleavage fragments resolved by MALDI-MS. For each cysteine proteinase and SQN-5 mixture, a major peak was detected at ~4031 Da (Figure 6 and data not shown for catL and catS). These data confirmed that the cleaved RSL was 17 amino acids in length and that the Thr-Ser motif located at the canonical P1−P1′ site was indeed the reactive center for the interaction between SQN-5 and catK, -L, -S, and -V. Moreover, this result confirmed the importance of the P2 Leu residue in directing substrate-like cleavages by this group of papain-like cysteine proteinases. On several traces, a peak was also detected at ~4333 Da (Figure 6). This peak represents either an alternative cleavage site or possibly a

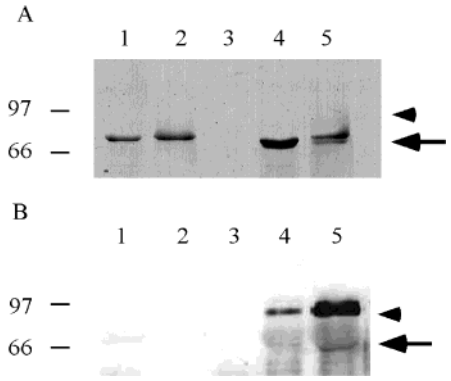

FIGURE 5: Formation of a complex between SQN-5 and cathepsin L. SCCA1 alone (4.0 μg, lane 1), SQN-5 alone (4.0 μg, lane 2), catL alone (1.6 μg, lane 3), SCCA1 (4.0 μg) with catL (1.6 μg) (lane 4), and SQN-5 (4.0 μg) with catL (1.6 μg) (lane 5) were incubated at 25 °C for 10 min and then heated at 95 °C for 5 min in 2% SDS loading buffer without β-mercaptoethanol. Protein mixtures were separated by SDS−PAGE. (A) Coomassie blue-stained gel. Positions of molecular weight (MW) markers are noted to the left of the gel. The locations of SCCA1 and SQN-5 (arrow) and the SCCA−catL and SQN-5−catL complexes (arrowhead) are indicated. The M_r values of SCCA1, SQN-5, and catL are ~71000, ~71000, and ~24000, respectively. (B) Proteins from a companion gel were transferred to nitrocellulose. Serpin−catL complexes were detected using a rabbit polyclonal catL antiserum as the primary antibody and a horseradish peroxidase-linked anti-rabbit antibody as the secondary antibody. The bands were detected by chemiluminescence.

spurious fragment derived from the original complex. Serpin−proteinase complexes are susceptible to cleavage by residual free enzyme (*27*−*29*).

Although the papain-like cysteine proteinases cleaved the RSL of SQN-5 between the Thr and Ser residues (Figure 6), it was unlikely that the serine proteinase, catG, would utilize the same motif. Since chymotrypsin-like serine proteinases cleave preferentially after aromatic (e.g., Phe or Tyr) or bulky hydrophobic (e.g., Leu or Val) residues, we predicted that catG would cleave SQN-5's RSL after the Leu residue positioned at the canonical P2 site. The MALDI-MS trace showed that this was not the case (Figure 6). CatG appeared to cleave the RSL of SQN-5 after the Val residue located in the canonical P4 position.

Table 2: Comparison of Second-Order Rate Constants (k_a) for the SQN-5 and SCCA1 Interactions with Papain-like Cysteine Proteinases[a]

proteinase	SQN-5	SCCA1	proteinase	SQN-5	SCCA1
catK	5.9	11[b]	catS	4.2	52[b]
catL	8.2	30[b]	catV	12.6	7.9

[a] Second-order rate constants (k_a) were determined under first- or second-order conditions as described in Experimental Procedures. All values are $\times 10^4$ M^{-1} s^{-1}. [b] These values were reported previously and are included to facilitate comparisons with SQN-5 (*5*).

Phylogenetic Relationship between SQN-5, SCCA1 (SERPINB3), SCCA2 (SERPINB4), and Other ov-Serpins. Data showing that SQN-5's inhibitory activity was comparable to those of both SCCA1 and SCCA2 prompted us to consider their phylogenetic relationship. To perform this analysis, we compared the amino acid sequences of all known human ov-serpins (SERPINB1−13), their putative mouse orthologs, and three additional unpublished SQN-like sequences (D. Askew and G. Silverman). The bootstrapped distance tree (Figure 7) demonstrated that SERPINB13, SERPINB3, SERPINB4, and the SQN cluster ($n = 4$) formed a well-supported (100%) subclade within the ov-serpin clade (*21*). Within this subclade, SERPINB3 and SERPINB4 as well as the SQN cluster

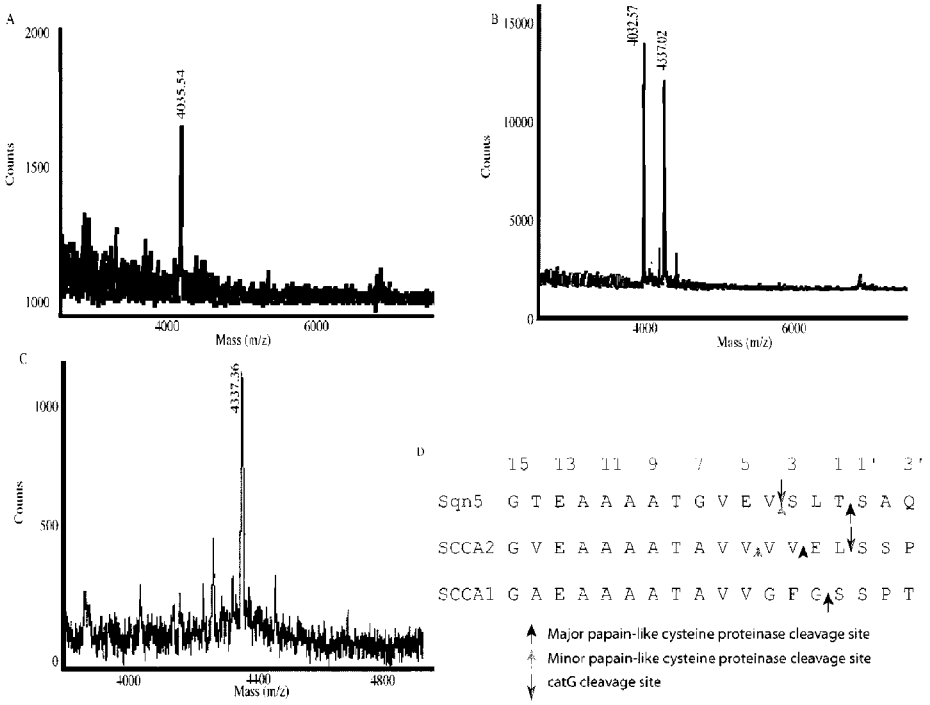

FIGURE 6: Cysteine proteinase cleavage sites in the RSL of SQN-5. For the cysteine proteinases, 1.2 μM enzyme in cathepsin buffer was mixed with 12 μM SQN-5. For catG, 2 μM proteinase in PBS reaction buffer was mixed with 2 μM SQN-5 for 5 min at 25 °C. The protein mixtures were then analyzed by MALDI-MS. (A) Representative trace from the MALDI-MS data for catK (A), catV (B), and catG (C). The arbitrary counts are plotted against the molecular mass. The peak corresponding to the ~4000 Da C-terminal cleavage product is labeled with the exact mass. (D) Schematic representation of the RSL cleavage sites of SQN-5 as compared to those previously published for SCCA1 and SCCA2 (*5*, *8*).

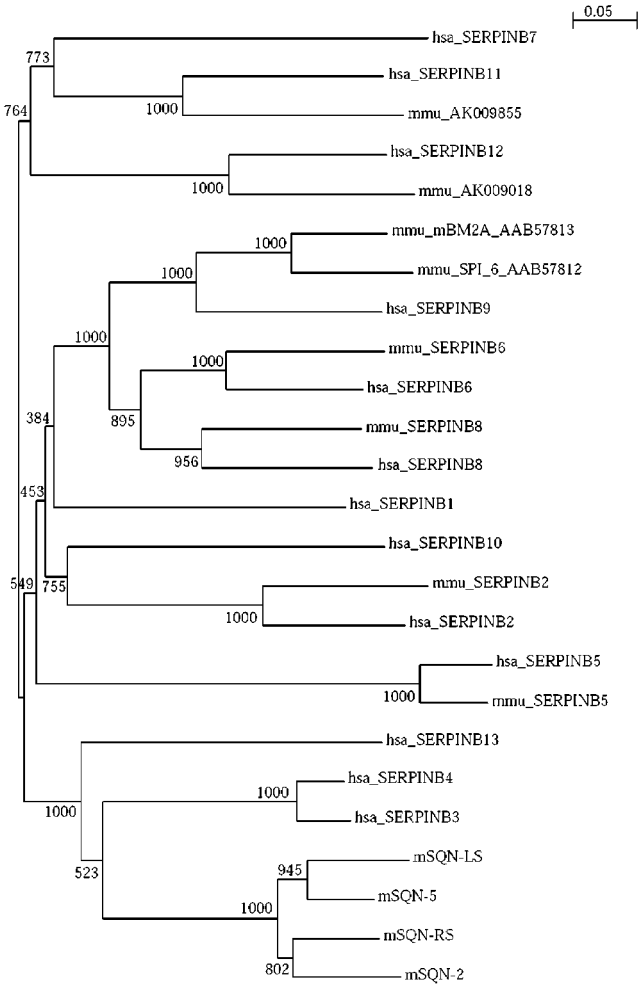

FIGURE 7: Unrooted distance tree depicting the phylogenetic relationships between mouse and human ov-serpins. Bootstrap values of >950 represent statistically significant nodes (*46*). The bar indicates the number of substitutions per 100 amino acids.

formed two discrete well-supported (100%) groups (Figure 7). The precise order of divergence between SERPINB13 and either the SERPINB3/SERPINB4 group or the SQN group was unclear as this node was poorly supported (52.3%).

While the SQNs were more closely related to the SCCAs then any other ov-serpins, the timing of their divergence had not been determined. Easteal, Collet, and Betty (*30*) estimate that rodents and primates diverged approximately 122 million years ago. By calculating divergence times from multiprotein sequences for several mammalian species, Nei and Glazko also estimate the distance to be approximately 96 million years (*31*). To calibrate the "molecular clock", we calculated the average evolutionary rate based on differences between orthologous mouse and human ov-serpins (i.e., SERPINB5, SERPINB6, SERPINB8, and SERPINB2) relative to their common ancestor. On the basis of this calculated rate of 0.98% accepted mutations (PAM) per million years, the average distance from SERPINB3 and SERPINB4 to their common ancestor (4.2 PAM) suggested that the duplication event occurred approximately 42 million years ago (MYA). The SQN-2 and SQN-RS pair diverged approximately 84 MYA, and the SQN-5 and SQN-LS pair diverged approximately 72 MYA. The two pairs themselves diverged approximately 100 MYA. Finally, the SQNs and SCCA1/2 diverged ~250−280 MYA.

DISCUSSION

On the basis of similar expression patterns, equivalent gene structure, a high degree of amino acid sequence conservation, and chromosomal synteny, we predicted that SQN-5 was the murine ortholog of the human serpin, SCCA2 (SERPINB4), or the adjacent and nearly identical serpin, SCCA1 (SERPINB3) (*11*). Since both SQN-5 and SCCA2 inhibit catG and mast cell chymase, whereas SCCA1 neutralizes the papain-like cysteine proteinases catK, -L, and -S (*5*, *8*, *11*), it appeared that SQN-5 was *Scca2*. However, the results from this study indicated that SQN-5's inhibitory profile was broader than that originally reported. SQN-5 was found to be a potent inhibitor of the papain-like cysteine proteinases catK, -L, and -S. In addition, both SQN-5 and SCCA1 inhibited the recently discovered papain-like cysteine proteinase, catV (*14*). Although recent assays using high concentrations of inhibitor and enzyme show that SCCA2 also can serve as a cysteine proteinase inhibitor, the second-order rate constant for this reaction is 50-fold lower than that measured for either the SCCA1− or SQN5−cysteine proteinase interactions (*9*). Thus, SQN-5's inhibitory profile resembles those of both SCCA1 and SCCA2.

To our knowledge, SQN-5 is the first serpin identified that had dual mechanistic-class reactivity with respect to chymotrypsin-like serine proteinases and papain-like cysteine proteinases. This dual reactivity was characterized by (1) comparable second-order rate constants ($>10^4$ M^{-1} s^{-1}), (2) stoichiometries of inhibition that were nearly 1:1, and (3) the use of overlapping reactive centers within the RSL. Since these targets use different active site architectures to degrade a different array of substrates, it was not surprising to find that SQN-5 employed different reactive centers to inhibit two structurally distinct classes of proteinases. Although the papain-like cysteine proteinases cleaved after the Thr residue in the canonical P1 position, catG cleaved after the Val residue located in the canonical P4 position. The location of this cleavage site was unusual in that it would generate an N-terminal RSL of only 14 residues (see below). However, it is interesting to note that catG cleaved the RSLs of both SQN-5 and SCCA2 after hydrophobic residues (Val and Leu, respectively) preceded by a Glu residue. The importance of Glu in this position was shown by detecting a decrease in the k_a of >50% for the SCCA2−catG interaction when this residue was changed to a Gly (*9*).

The use of overlapping reactive centers to inhibit two different types of serine proteinases was observed with α2-antiplasmin (SERPINF2) (*32*, *33*) and C1-inhibitor (SERPING1) (*34*). More recently, five human ov-serpins [macrophage neutrophil elastase inhibitor (SERPINB1) (*35*), SCCA2 (SERPINB4) (*9*), PI6 (SERPINB6) (*36*), PI8 (SERPINB8) (*37*), and PI9 (SERPINB9) (*38*)] were found to use overlapping reactive centers within their RSLs to inhibit different types of serine proteinases (summarized in Table 3). What is striking about this cleavage site data is the varying length of the N-terminal portions of the cleaved reactive site loops. Most cleaved reactive site loops are 17 residues in length starting from the highly conserved Glu residue located in the proximal hinge region (P17 of the canonical serpin, α1-antitrypsin, SERPINA1). An explanation for this length

Table 3: Cleavage Sites in the Reactive Site Loops of Serpins with Overlapping Reactive Centers[i]

	reactive site loop:																		
Serpin	17	16	15	14	13	12-9	8	7	6	5	4	3	2	1	1′	2′	3′	4′	5′	Ref
a2-AP (SEPINF2)	E	V	G	V	E	A	T	S	I	A	M[a]	S	R[b,c]	M[a]	S	L	S	S	F	(*32*, *33*)
C1-inhibitor (SERPING1)	E	T	G	V	E	A	S	A	I	S	V	A[a]	R[d]	T	L	L	V	F	E	(*47*)
MNEI (SERPINB1)	E	E	G	T	E	A	T	A	G	I	A	T	F[a]	C[e]	M	L	M	P	E	(*35*)
SCCA2 (SERPINB4)	E	E	G	V	E	A	T	A	V	V	V	V[f]	E	L[g]	S	S	P	S	T	(*9*)
PI6 (SERPINB6)	E	E	G	T	E	A	T	A	A	I	M	M	M[a]	R[e]	C	A	R	F	V	(*36*)
PI8 (SERPINB8)	E	E	G	T	E	A	T	A	V	V	R	N	S	R[e]	C	S[a]	R	M	E	(*37*)
PI9 (SERPINB9)	E	E	G	T	E	A	S	S	C	F	V	V	A	E[h]	C	C[e]	M	E	S	(*38*)
SQN5	E	E	G	T	E	A	T	G	V	E	V[g]	S	L	T[f]	S	A	Q	I	A	

[a] Cleavage sites (vertical bar) for chymotrypsin. [b] Cleavage sites (vertical bar) for plasmin. [c] Cleavage sites (vertical bar) for trypsin. [d] Cleavage sites (vertical bar) for factor XII. [e] Cleavage sites (vertical bar) for human neutrophil elastase. [f] Cleavage sites (vertical bar) for catS. [g] Cleavage sites (vertical bar) for catG. [h] Cleavage sites (vertical bar) for granzyme B. [i] The numbering of the reactive site loop is based on the canonical sequence of α1-antitrypsin (SERPINA1).

requirement is provided in an elegant study by Zhou et al. (*26*), in which they studied the effects of adding or deleting residues between the P1 residue and the RSL hinge region of α1-antitrypsin Pittsburgh. When the RSL was lengthened to 18 or 19 residues, the stability of the serpin−proteinase complex was reduced dramatically. Shortening the RSL to 15 or 16 residues decreased the efficiency of inhibition (the SI increased), but the stability of the complex was increased. Further shortening of the RSL to 14 residues resulted in a loss of detectable serpin−proteinase complexes. On the basis of the mechanistic model of proteinase inhibition, where RSL insertion exerts torque on the active site after pulling the proteinase up against the body of the serpin, the RSL length would be expected to alter complex stability by modulating the degree of "plucking stress" and distortion placed on the active site architecture (*26*). If the RSL is too long, less stress is applied, the active site architecture is maintained, and the proteinase dissociates from the serpin. In contrast, if the RSL is shortened, plucking stress increases, active site architecture is distorted, and the proteinase remains covalently bound to the serpin. However, further shortening the RSL would slow or possibly inhibit loop insertion due to steric clashes between β-sheet A and the proteinase. On the basis of the RSL cleavage data summarized in Table 3, the length of the N-terminal RSL that permits inhibitory function can vary between 14 (SQN5 and possibly SERPINF2) and 19 (SERPINB8 and -9) residues. Although this range is slightly larger than that predicted by the α1-antitrypsin Pittsburgh mutants (15−19 residues), viable RSL length may depend on the proteinase−serpin pair.

While there are now multiple examples of serpins using overlapping reactive centers to inhibit two or more types or serine proteinases, there are currently only a few examples of dual mechanistic-class inhibitors. SERPINB9 inhibits the serine proteinase granzyme B (*39*) and possibly members of another structurally distinct family of cysteine proteinases, the caspases (*2*). However, the inability to detect RSL cleavage and a second-order rate constant on the order of $\sim 10^2$ M^{-1} s^{-1} suggest that the inhibition of caspase-1 may not involve a typical "irreversible" serpin suicide substrate mechanism (reviewed in ref *1*). SCCA1 and most likely SQN-5 employ a typical serpin inhibitory mechanism to inhibit papain-like cysteine proteinases (*9*). Regardless of the mechanisms, the ability of at least some serpins to inhibit proteinases from more that one mechanistic class suggests that these serpins may have evolved to regulate enzymes involved in parallel or intersecting catalytic cascades. In the case of SERPINB9, the inhibition of granzyme B and caspase-1 shows that this serpin is capable of regulating certain programmed cell death pathways (*39*). In the case of SQN-5, the biological importance of inhibiting both chymotrypsin-like enzymes and lysosomal cysteine proteinases is less apparent. Conceivably, this serpin regulates the degradation of extracellular matrix components or protects

the cytosol from the adventitious proteinases that leak from membrane-bound organelles such as secretory granules, lysosomes, or endosomes (*40*−*42*).

Although SQN5 is closely related to both SCCA1 and SCCA2 (*11*), the biochemical activity presented in this study underscores their evolutionary relatedness. However, a more detailed phylogenetic analysis using mouse and human ov-serpin amino acid sequences recently made available showed that the evolutionary relationship between the SQNs and the SCCAs was more complex than those of most other mouse−human ov-serpin pairs. The SQNs and SCCAs evolved from a common ancestral SQN/SCCA-like gene ∼250−280 MYA. If this approximation is correct, then this duplication event would have occurred after the split between birds and mammals but well before the rodent and human radiation that occurred 90−120 MYA (*30*, *31*). In this scenario, we might expect to find higher-homology level SQN-like genes in humans and SCCA-like genes in mice. However, this does not appear to be the case. While we cannot exclude the presence of SCCA-like genes in mice at this time, the relative completeness of the human genome virtually precludes the existence of SQN-like genes in humans. These findings would suggest that the SQNs and SCCAs evolved from a common ancestor, but there was reciprocal loss of these genes in humans and mice, respectively. Alternatively, several studies have shown that the rate of mutation for certain mouse serpins is exceptionally high (*43*−*45*). If this were the case for the SQNs, then the estimated time of divergence between the SQNs and SCCAs was significantly less than that predicted and may have occurred closer to the divergence between rodents and humans. In turn, local duplication events and positive selection would then account for the expansion of the SCCA and SQN genes in their respective species. Regardless of the scenario, it appears that the SQNs and SCCAs are paralogous genes derived from an ancestor that was endowed with both serine and cysteine proteinase inhibitory activity. Biochemical analysis of serpins from organisms up and down the evolutionary tree should help determine whether this is the case and if dual-class inhibitors are more pervasive within the serpin superfamily than has been appreciated.

REFERENCES

1. Silverman, G. A., Bird, P. I., Carrell, R. W., Coughlin, P. B., Gettins, P. G., Irving, J. I., Lomas, D. A., Luke, C. J., Moyer, R. W., Pemberton, P. A., Remold-O'Donnell, E., Salvesen, G. S., Travis, J., and Whisstock, J. C. (2001) *J. Biol. Chem. 276*, 33293−33296.
2. Annand, R. R., Dahlen, J. R., Sprecher, C. A., De Dreu, P., Foster, D. C., Mankovich, J. A., Talanian, R. V., Kisiel, W., and Giegel, D. A. (1999) *Biochem. J. 342* (Part 3), 655−665.
3. Komiyama, T., Ray, C. A., Pickup, D. J., Howard, A. D., Thornberry, N. A., Peterson, E. P., and Salvesen, G. (1994) *J. Biol. Chem. 269*, 19331−19337.
4. Hook, V. Y., Purviance, R. T., Azaryan, A. V., Hubbard, G., and Krieger, T. J. (1993) *J. Biol. Chem. 268*, 20570−20577.
5. Schick, C., Pemberton, P. A., Shi, G.-P., Kamachi, Y., Cataltepe, S., Bartuski, A. J., Gornstein, E. R., Bromme, D., Chapman, H. A., and Silverman, G. A. (1998) *Biochemistry 37*, 5258−5266.
6. Schick, C., Bromme, D., Bartuski, A. J., Uemura, Y., Schechter, N. M., and Silverman, G. A. (1998) *Proc. Natl. Acad. Sci. U.S.A. 95*, 13465−13470.
7. Schneider, S. S., Schick, C., Fish, K. E., Miller, E., Pena, J. C., Treter, S. D., Hui, S. M., and Silverman, G. A. (1995) *Proc. Natl. Acad. Sci. U.S.A. 92*, 3147−3151.
8. Schick, C., Kamachi, Y., Bartuski, A. J., Cataltepe, S., Schechter, N. M., Pemberton, P. A., and Silverman, G. A. (1997) *J. Biol. Chem. 272*, 1849−1855.
9. Luke, C., Schick, C., Tsu, C., Whisstock, J. C., Irving, J. A., Bromme, D., Juliano, L., Shi, G. P., Chapman, H. A., and Silverman, G. A. (2000) *Biochemistry 39*, 7081−7091.
10. Kato, H. (1992) in *Serological Cancer Markers* (Sell, S., Ed.) pp 437−451, Humana Press, Totowa, NJ.
11. Bartuski, A. J., Kamachi, Y., Schick, C., Massa, H., Trask, B. J., and Silverman, G. A. (1998) *Genomics 54*, 297−306.
12. Bromme, D., Bonneau, P. R., Lachance, P., and Storer, A. C. (1994) *J. Biol. Chem. 269*, 30238−30242.
13. Bromme, D., Bonneau, P. R., Lachance, P., Wiederanders, B., Kirschke, H., Peters, C., Thomas, D. Y., Storer, A. C., and Vernet, T. (1993) *J. Biol. Chem. 268*, 4832−4838.
14. Bromme, D., Li, Z., Barnes, M., and Mehler, E. (1999) *Biochemistry 38*, 2377−2385.
15. Salvesen, G., and Nagase, H. (1989) in *Proteolytic enzymes: A practical approach* (Beynon, R. J., and Bond, J. S., Eds.) pp 83−104, IRL Press, Oxford, U.K.
16. Morrison, J. F., and Walsh, C. T. (1988) *Adv. Enzymol. Relat. Areas Mol. Biol. 61*, 201−301.
17. Beatty, K., Bieth, J., and Travis, J. (1980) *J. Biol. Chem. 255*, 3931−3934.
18. Laemmli, U. K. (1970) *Nature 227*, 680−685.
19. Silverman, G. A., Yang, E., Proffitt, J. H., Zutter, M., and Korsmeyer, S. J. (1993) *Mol. Cell. Biol. 13*, 5469−5478.
20. Thompson, J. D., Higgins, D. G., and Gibson, T. J. (1994) *Nucleic Acids Res. 22*, 4673−4680.
21. Irving, J. A., Pike, R. N., Lesk, A. M., and Whisstock, J. C. (2000) *Genome Res. 10*, 1845−1864.
22. Perriere, G., and Gouy, M. (1996) *Biochimie 78*, 364−369.
23. Travis, J., and Salvesen, G. S. (1983) *Annu. Rev. Biochem. 52*, 655−709.
24. Gettins, P., Patston, P. A., and Schapira, M. (1992) *Hematol. Oncol. Clin. North Am. 6*, 1393−1408.
25. Longas, M. O., and Finlay, T. H. (1980) *Biochem. J. 189*, 481−489.
26. Zhou, A., Carrell, R. W., and Huntington, J. A. (2001) *J. Biol. Chem. 276*, 27541−27547.
27. Egelund, R., Petersen, T. E., and Andreasen, P. A. (2001) *Eur. J. Biochem. 268*, 673−685.
28. Kaslik, G., Patthy, A., Balint, M., and Graf, L. (1995) *FEBS Lett. 370*, 179−183.
29. Stavridi, E. S., O'Malley, K., Lukacs, C. M., Moore, W. T., Lambris, J. D., Christianson, D. W., Rubin, H., and Cooperman, B. S. (1996) *Biochemistry 35*, 10608−10615.
30. Easteal, S., Collet, C. C., and Betty, D. J. (1995) *The Mammalian Molecular Clock*, R. G. Landes Co., Austin, TX.
31. Nei, M., Xu, P., and Glazko, G. (2001) *Proc. Natl. Acad. Sci. U.S.A. 98*, 2497−2502.
32. Enghild, J. J., Valnickova, Z., Thogersen, I. B., Pizzo, S. V., and Salvesen, G. (1993) *Biochem. J. 291*, 933−938.
33. Potempa, J., Shieh, B.-H., and Travis, J. (1988) *Science 241*, 699−700.
34. Aulak, K. S., Eldering, E., Hack, C. E., Lubbers, Y. P., Harrison, R. A., Mast, A., Cicardi, M., and Davis, A. E. d. (1993) *J. Biol. Chem. 268*, 18088−18094.
35. Cooley, J., Takayama, T. K., Shapiro, S. D., Schechter, N. M., and Remold-O'Donnell, E. (2001) *Biochemistry 40*, 15762−15770.
36. Riewald, M., and Schleef, R. R. (1996) *J. Biol. Chem. 271*, 14526−14532.
37. Dahlen, J. R., Foster, D. C., and Kisiel, W. (1998) *Biochem. Biophys. Res. Commun. 244*, 172−177.
38. Dahlen, J. R., Foster, D. C., and Kisiel, W. (1999) *Biochim. Biophys. Acta 1451*, 233−241.
39. Bird, C. H., Sutton, V. R., Sun, J., Hirst, C. E., Novak, A., Kumar, S., Trapani, J. A., and Bird, P. I. (1998) *Mol. Cell. Biol. 18*, 6387−6398.
40. Page, L. J., Darmon, A. J., Uellner, R., and Griffiths, G. M. (1998) *Biochim. Biophys. Acta 1401*, 146−156.

41. Rodriguez, A., Webster, P., Ortego, J., and Andrews, N. W. (1997) *J. Cell Biol. 137*, 93−104.
42. Griffiths, G. M. (1996) *Trends Cell Biol. 6*, 329−332.
43. Borriello, F., and Krauter, K. S. (1991) *Proc. Natl. Acad. Sci. U.S.A. 88*, 9417−9421.
44. Hill, R. E., and Hastie, N. D. (1987) *Nature 326*, 96−99.
45. Rheaume, C., Goodwin, R. L., Latimer, J. J., Baumann, H., and Berger, F. G. (1994) *J. Mol. Evol. 38*, 121−131.
46. Felsenstein, J. (1996) *Methods Enzymol. 266*, 418−427.
47. Aulak, K. S., Davis, A. E., III, Donaldson, V. H., and Harrison, R. A. (1993) *Protein Sci. 2*, 727−732.

BI015999X